JARS Journal of Applied Remote Sensing

RESEARCH PAPER

Remote sensing to predict soil moisture tension in water saving rice systems of temperate South-Eastern Australia

Matthew Champness,* Carlos Ballester Lurbe, Rodrigo Filev Maia, and John Hornbuckle

Deakin University, School of Life and Environmental Science, Centre for Regional and Rural Futures, Griffith, New South Wales, Australia

ABSTRACT. Non-ponded aerobic rice offers the opportunity for substantial global savings of irrigated water. Site and environment specific soil tension thresholds have been identified for non-ponded rice production to save water without adverse yield consequences. However, soil tension readings are point-source measures that are not necessarily representative of a given irrigation area/paddy and become costly when required in each paddy. Remote sensing offers spatial advantages and has been demonstrated in many crops to accurately estimate crop evapotranspiration (ETc), which is often used to schedule irrigation. This study uses soil moisture tension (SMT) data measured in a commercial aerobic rice experiment conducted in temperate Australia on a heavy clay soil to demonstrate the relationship between soil tension and remotely sensed estimated cumulative ETc between irrigation events using open access satellite imagery. The model was used to predict SMT in the second growing season during the vegetative period after establishment until PI with a root mean squared error of ±5.8 kPa. This demonstrates the ability of irrigators to schedule irrigation in water saving rice using open satellite-derived data that can be incorporated into an automated irrigation system, without the need for costly in-field soil moisture sensors. Future research to integrate forecast crop evapotranspiration could enable soil moisture forecasting days in advance, providing irrigators more time to plan irrigation activities.

 [DOI: 10.1117/1.JRS.17.044501]

Keywords: *Oryza sativa*; normalized difference vegetation index; crop evapotranspiration; irrigation; aerobic rice

Paper 230116G received Mar. 27, 2023; revised Aug. 29, 2023; accepted Sep. 18, 2023; published Oct. 3, 2023.

1 Introduction

Rice cultivation strategies that reduce or eliminate the period of permanent flooding have been demonstrated to significantly reduce irrigated rice water use,[1–12] paddy rice methane emissions,[13–16] and arsenic concentrations.[3,16] However, a higher degree of irrigation management and infrastructure is required at both the farm and system levels, when compared with continuously flooded rice.[17] In areas with timely capacity to control irrigation water, knowledge of when to initiate irrigation is required to avoid detrimental water stress. Extensive research has been conducted to determine the extent of soil moisture deficit to optimize water productivity (the amount of crop produced per unit of water) in alternate wetting and drying (AWD), in which water levels decline below the soil surface prior to shallow reflooding, and aerobic rice in which

*Address all correspondence to Matthew Champness, m.champnesss@deakin.edu.au

rice is grown in the absence of flooded/permanent water. The water table depth and soil moisture deficit are the most widely used parameters to initiate irrigation in such water saving cultivation techniques.

Soil moisture tension (SMT) refers to how tightly water is held to the soil and is measured in units of pressure (kPa). Values higher than −10 kPa indicate saturated soil, with increasingly negative numbers referring to increasing tension and energy required for the plant to extract water. Irrigation to maintain rootzone ***SMT > −10 kPa is believed to not adversely affect rice yields.[18] However, suitable equipment to monitor SMT is often not available for many farmers. As such, "AWD safe" has been recommended by the International Rice Research Institute; this involves applying irrigation when the perched water table (measured by in-field water tubes/pani-pipes) falls to 15 cm below the soil surface.[19] This threshold was devised to ensure no yield penalties. However, irrigation thresholds varying from −10 kPa to beyond −90 kPa have been demonstrated in aerobic and AWD rice to maintain yields comparable to that of flooded rice.[4,5,9,10,20–22] Such variability in irrigation thresholds exist as a result of the duration and frequency of water stress, ground water table, cultivar selection, and environmental conditions.[1,5,23] These aforementioned characteristics and the management objectives (maximizing water productivity, yield, quality, labor input, etc.) will determine the irrigation regime. Therefore, in certain environments and conditions, it may be possible to extend SMT beyond the conservative "safe" limit. However, water and heat stress during the reproductive period often result in yield decline;[5,24] therefore, the research presented here focuses on the vegetative period.

Although soil moisture sensors have been used in commercial settings to schedule irrigation in rice,[25] point-source measures provide poor spatial replication, with commercial farms requiring multiple sensors per field, adding significant cost.[26,27] Further, soil cracking around the sensor, particularly in heavy clay soils, can limit the reliability of sensor data.[28] Remote sensing can offer spatial advantages over point-based sensing in field sensors and has been demonstrated to estimate soil moisture; however, the accuracy of the direct estimation of soil moisture for irrigation scheduling requires improvements, according to Liang and Wang.[29] Although not yet developed to accurately estimate soil moisture for irrigation scheduling at a sub-paddock level, remote sensing to estimate crop evapotranspiration (ETc), which is then used to schedule irrigation in broadacre agriculture, is well established, e.g., IrriSAT and evapotranspiration flux (EEFLUX).[30,31] Using the FAO56 approach explained in more detail in Allen et al., crop water need, known as ETc, is calculated as a product of reference evapotranspiration (ET_0) and a crop coefficient (k_c), as given in the following equation:[32]

$$\mathrm{ETc} = \mathrm{ET}_0 \times k_c. \tag{1}$$

ET_0 refers to the rate of evaporation of actively growing well-watered grass of uniform height (12 cm) that completely shades the ground of a large area with a fixed surface resistance.[32] Thus, ET_0 is only dependent on climatic factors that can be measured by a weather station. k_c is used to account for the crop factors such as ground cover, crop architecture, and aerodynamic resistance under standard conditions.[32] k_c is invariably difficult and costly to measure at a sub-paddock basis; however, it can be estimated using high spatial and temporal resolution remote sensed data to calculate vegetation indices. Specifically, the normalized difference vegetation index (NDVI) is linearly correlated to k_c.[33] This approach is often used in drop/sprinkler irrigated perennial crops with irrigators using estimated ETc thresholds since last irrigation to schedule irrigation and determine the quantity of irrigation water required.[34,35] Further, in broadacre surface irrigation, growers of crops such as wheat and cotton use cumulative ETc as calculated by remote sensed decision support tools, such as IrriSAT and EEFLUX, to schedule irrigation.[30,31] However, this is not currently possible in rice as ETc irrigation thresholds for water saving rice are not known, nor is the relationship between ETc and SMT in water saving rice systems despite[36] reporting a relationship between in-field sensed SMT and satellite derived ETc between irrigation events in cotton.

SMT decline during non-ponded periods of rice cultivation is hypothesized to be correlated to the cumulative ETc between irrigation events. However, due to the changing nature of soil water loss throughout the season resulting from increased canopy cover, it is further theorized that the elapsed time and therefore the cumulative ETc after an irrigation event at which this relationship commences will change throughout the season. Determination of such a relationship

and accounting for seasonal variation could enable SMT to be predicted and used to schedule irrigation, without the requirement for multiple costly in-field sensors.

Using data from a commercial aerobic rice experiment in southern Australia with various soil moisture deficits imposed in the vegetative period,[25] this study aims to build and validate a model to predict SMT during the vegetative stage of rice grown aerobically (under non-ponded conditions) using measured (i) SMT data, (ii) weather conditions, and (iii) NDVI-based remotely sensed crop coefficients. Specifically, the study aimed to use commercially available open access remote sensed data sources to develop and test such a model to showcase the opportunity for rice growers and industry to implement the model with minimal barriers to adoption. However, the environmental and site-specific nature of such thresholds may limit its applicability across different regions. Nevertheless, such a model offers potential to be incorporated into an automated gravity surface irrigation system, providing remote irrigation control. This has the potential to provide confidence and assist farmers in adopting a water saving rice culture.

2 Materials and Methods

2.1 Site Description

The study was conducted during two rice-growing seasons (2020/2021 and 2021/2022) on a commercial property in the Murrumbidgee Valley near Griffith in South-Eastern Australia (34°17′18″ S, 146°03′03″ E). The soil is a typical rice growing soil in the region, classified as a self-mulching clay with a 30 cm brown A horizon over a dense red B horizon.[37] The 0 to 15 cm soil consists of 34% sand, 9% silt, and 56% clay, as reported in Ref. 25. The climate is characterized as temperate, with hot dry summers and low humidity. Mean annual rainfall is 385 mm for Griffith with a typical in-season rainfall of 150 mm and evapotranspiration of 1150 mm.[38] The monthly rainfall and mean daily ET_0 (mm) for the two growing seasons when the study was conducted are presented in Fig. 1.

The field, which is shown in Fig. 2, was a 9-bay/replicate, down the grade border-check layout (34 ha) with replicates 500 to 600 m in length and 50 to 75 m wide (~3.5 ha each). Earthen banks 30 cm high were used to separate replicates. Irrigation water was supplied at the top of the replicate using lay-flat rubber stops controlled using portable automated self-powered AutowichPro's (Padman Automation, Strathmerton, VIC, Australia). The timing of the first two-three irrigation events was based on agronomic and herbicide requirements to guarantee good rice establishment prior to the installation of soil moisture sensors for monitoring and irrigation decisions. Subsequently, various irrigation deficits were investigated during the remainder of the vegetative period until panicle initiation. Irrigation and agronomic information are detailed in Ref. 25. In brief, short-season semi-dwarf c.v. Viand was sown at a rate of 130 and

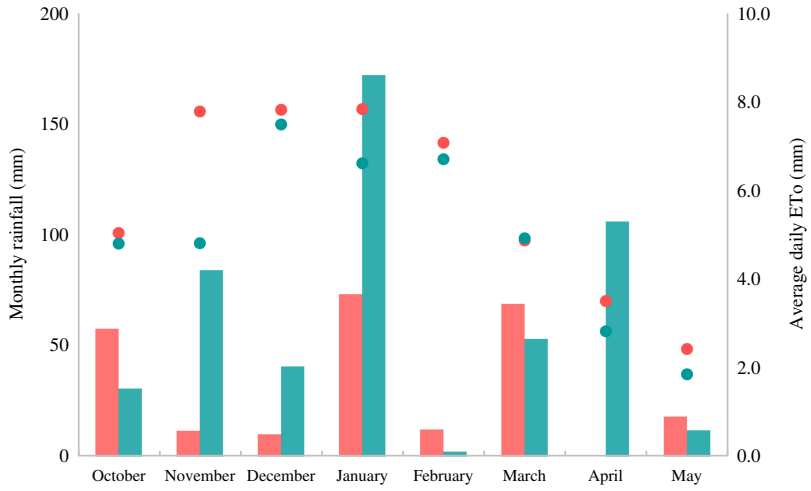

Fig. 1 Monthly rainfall (mm) represented by vertical bars on the left axis and daily average ET_0 (mm) represented as dots on the right axis during the cropping seasons of 2020–2021 (year 1; red) and 2021–2022 (year 2; blue) at Griffith, NSW.

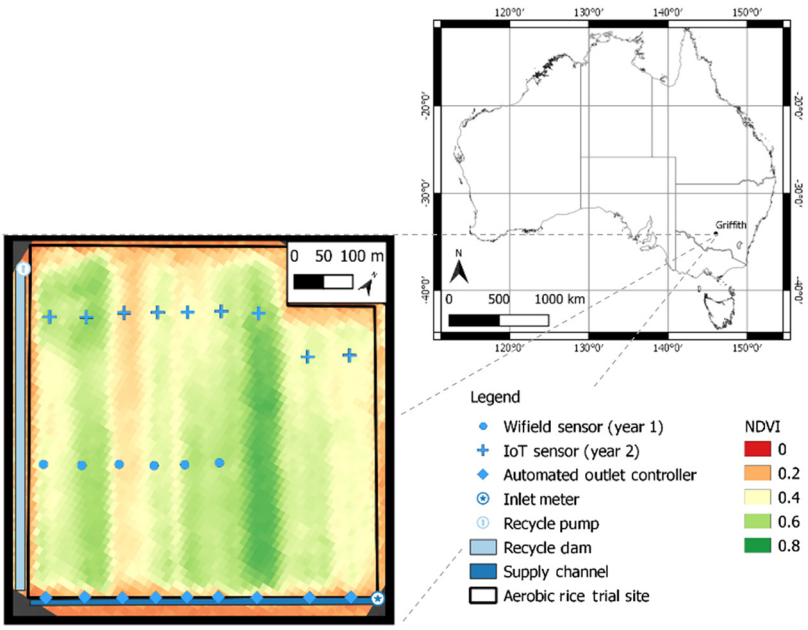

Fig. 2 Location of the commercial field site where the 2-year study was conducted with NDVI from 06/01/2021 (year 1).

120 kg/ha into wheat stubble and bare ground in years 1 and 2, respectively. Nitrogen was applied as granular urea (46% N) at a rate of 220 kg N/ha in a three-way split. SMT was measured using two watermark sensors (Model 200SS, Irrometer Company inc., Riverside, California, United States) to average results per replicate. Sensors were installed beside plants after establishment to ensure rootzone SMT was measured at a depth of 15 cm below ground. In year 1, sensors were connected to WiField loggers that offer low cost, low power data collection, storage, and transmission to the Google Cloud Platform in real time using an on-farm Wi-Fi network.[39] In the second year, solar powered LoRaWAN IoT communication stations (SensorPro's, Padman Automation, Strathmerton, VIC, Australia) were used to collect and send soil moisture data to the Padman Automation platform for real-time monitoring. SMT data presented in this manuscript are from four replicates in year 1 and five replicates in year 2 in which treatments aimed not to surpass either −15 kPa or −40 kpa during the vegetative period from establishment until panicle initiation as such an irrigation regime was reported by Ref. 25 to achieve sound water productivity without detrimentally delaying crop development.

2.2 Crop Evapotranspiration Estimation

Crop evapotranspiration (ETc) was estimated using the FAO56 method,[32] with water requirements calculated as the product of reference evapotranspiration (ET_0) and a crop coefficient as detailed previously in Eq. (1). Hourly reference evapotranspiration and rainfall were calculated from nearby weather stations using the standardized American Society of Civil Engineers equation. [40] Hourly data were used due to the effect that the time of day of irrigation may have in regard to ET_0. Crop coefficients were derived using IrriSAT[30] (temporal (~8 days) and spatial (10 × 10 m) resolution), which use Eq. (2) to estimate the actual crop coefficient from satellite multispectral images as[33]

$$k_c = 1.37 \times \mathrm{NDVI} - 0.086. \tag{2}$$

Canopy cover was hypothesized to influence the period after an irrigation event at which soil transitioned from a saturated to a non-saturated state. Remote sensed images to measure canopy cover were obtained from cloud-free Sentinel-2 satellite images every 3-4 days with a pixel resolution of 10 m and top of atmosphere reflectance during both growing seasons. The GeoTIFF images of the whole field site were processed in QGIS (Version 3.10), where polygons of 900 m^2 were created at the site of the soil moisture loggers. The zonal statistics tool available in

QGIS was used to obtain the mean and standard deviation data for each band at each polygon and used to compute NDVI[41] using Eq. (3), where R represents reflectance at the specific wavelength

$$\mathrm{NDVI} = \frac{R_{760} - R_{670}}{R_{760} + R_{670}} = \frac{\mathrm{Band8} - \mathrm{Band4}}{\mathrm{Band8} + \mathrm{Band4}}. \tag{3}$$

2.3 Model Creation and Validation

The model to estimate SMT (presented later in Sec. 3.2) was created using year 1 data from four-replicates and validated using data from five independent replicates collected in year 2. To evaluate the model performance, the coefficient of determination (R^2) and root mean squared error (RMSE) were calculated rather than the percentage error as the percentage can be substantial for SMT near 0 kPa[42] but of little relevance. RMSE was calculated as per Eq. (4), where n is the number of data points, y_i is the i'th measurement, and $\hat{y}_i$ is the corresponding predicted measurement:

$$\mathrm{RMSE} = \sqrt{\sum_{i=0}^{n} \frac{(\hat{y}_\mathrm{i} - y_\mathrm{i})^2}{n}}. \tag{4}$$

To account for the high number of data points at or near 0 kPa, actual SMT data were segmented into three categories; 0 to −10 kPa, beyond −10 kPa, and overall, with RMSE calculated for each category.

3 Results and Discussion

3.1 Soil Moisture Tension and Crop Evapotranspiration

SMT during the vegetative stage in relation to the number of days since the pre-emergent (first) irrigation of the individual replicates investigated in this study in years 1 and 2 is presented on the left side of Figs. 3 and 4, respectively. In all cases, SMT returned to 0 kPa after an irrigation event, indicating that sufficient irrigation water was applied to refill the soil profile at the monitored depth. The extent of the soil moisture deficit can be seen to vary between replicates and years as a result of different irrigation thresholds under investigation (detailed in Champness et al.).[25] It was due to the possible influence of climatic variability between seasons that data was segmented by year with various deficits in a year to understand if a single model approach could be used. The estimated crop evapotranspiration (with rainfall subtracted) in relation to the number of days since the pre-emergent irrigation of each replicate in years 1 and 2 is presented on the right side of Figs. 3 and 4, respectively. ETc was reset to 0 mm at the time of irrigation or when significant rainfall was recorded.

The relationship between SMT and cumulative ETc since the last irrigation for each individual replicate in both years is shown in Fig. 5. When an irrigation event occurred, ETc values were reset to zero. Therefore, within each graph, each line of declining soil moisture represents an individual deficit event within that replicate. For this reason, for certain points on the x-axis (ETc) there are multiple points on the y-axis (STM). The slope of the individual lines in Fig. 5 represents the relationship between SMT and ETc.

The point of inflexion on the x-axis in Fig. 5, known hereafter as "c," represents the cumulative ETc when SMT began to decline (< -1 kPa). The value of c was not consistent between replicates or within replicates (Fig. 5). However, c generally increased within each respective replicate throughout the season. This can be seen in Fig. 6, demonstrating that the time taken for soil to transition from saturated to non-saturated conditions increased throughout the season. This is explained by relatively high soil evaporation rates experienced when little canopy cover exists and is exacerbated with readily available water at the surface immediately after an irrigation or rainfall event.[32] The rate of soil drying decreases over time as the vapor pressure at the soil surface nears that of the atmospheric vapor pressure.[43] As canopy cover increases throughout the season, an increasing proportion of soil moisture loss is attributed to transpiration and the rate of loss from evaporation decreases, however, not proportionally.[32] Therefore, increasing canopy cover reduces the initial rate of soil moisture

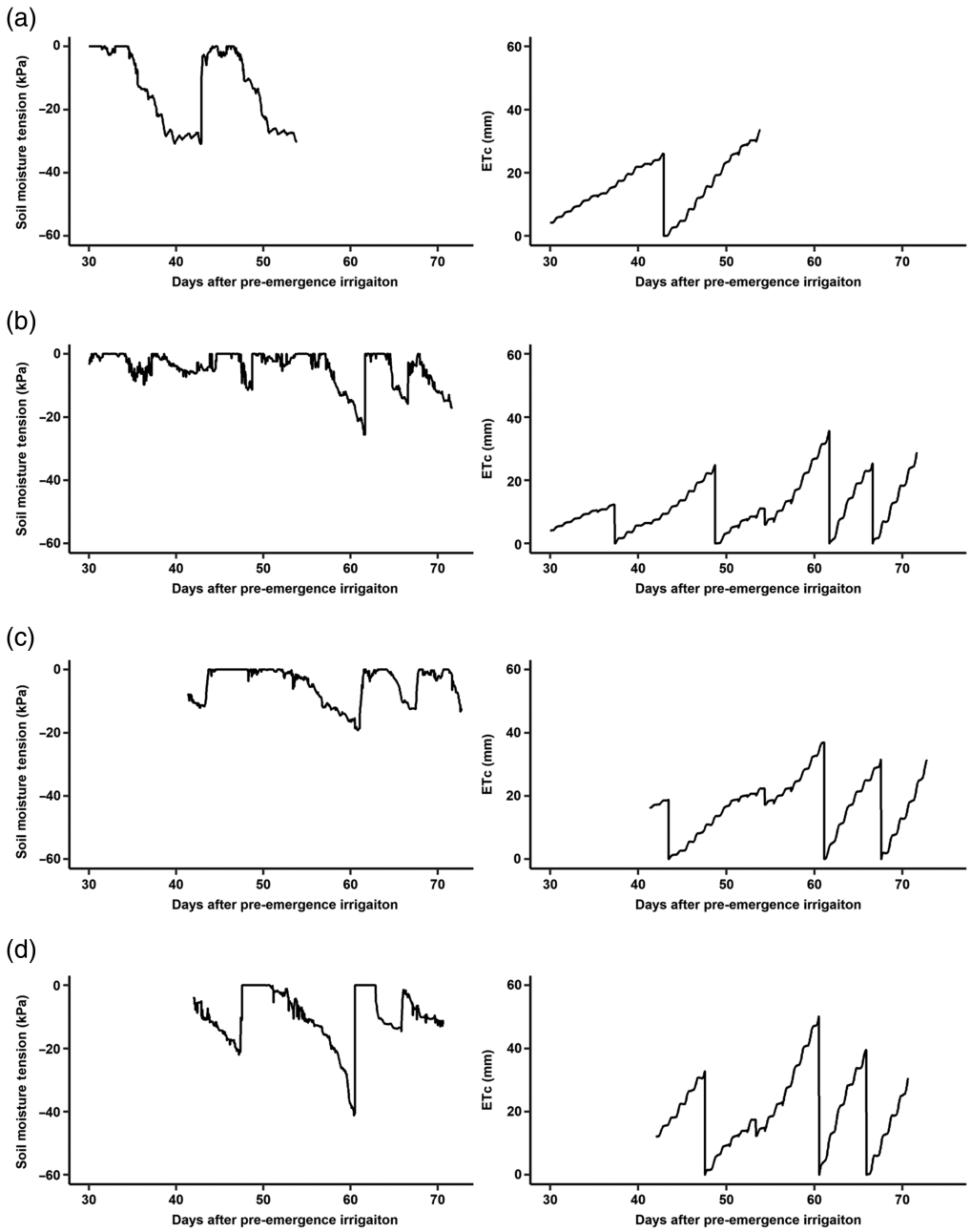

Fig. 3 Left: SMT (kPa) and right: ETc with rainfall subtracted (mm), in relation to number of days since pre-emergent irrigation with letters (a)–(d) used to distinguish individual replicate data from year 1. Note: IoT loggers to monitor SMT were not installed until establishment; hence data in the establishment phase is not presented, with logger issues in replicate "A" limiting the period that data was collected.

loss when compared with relatively bare soil, thus increasing the value of c as the rice continues to develop canopy closure.

3.2 Developing Model to Forecast Soil Moisture Tension

To determine the average relationship between SMT and ETc across all replicates in year 1, the x-axis of each deficit period for each replicate was translated c units horizontally to create an inflexion at zero [Fig. 7(a)]. In general, the gradient of the individual irrigation events in different replicates is somewhat similar, with an $R^2 = 0.71$. This demonstrates a relatively consistent soil moisture decline in relation to ETc throughout the period under investigation. This relationship would likely differ in different soil types or under a more severe irrigation regime as the rate of

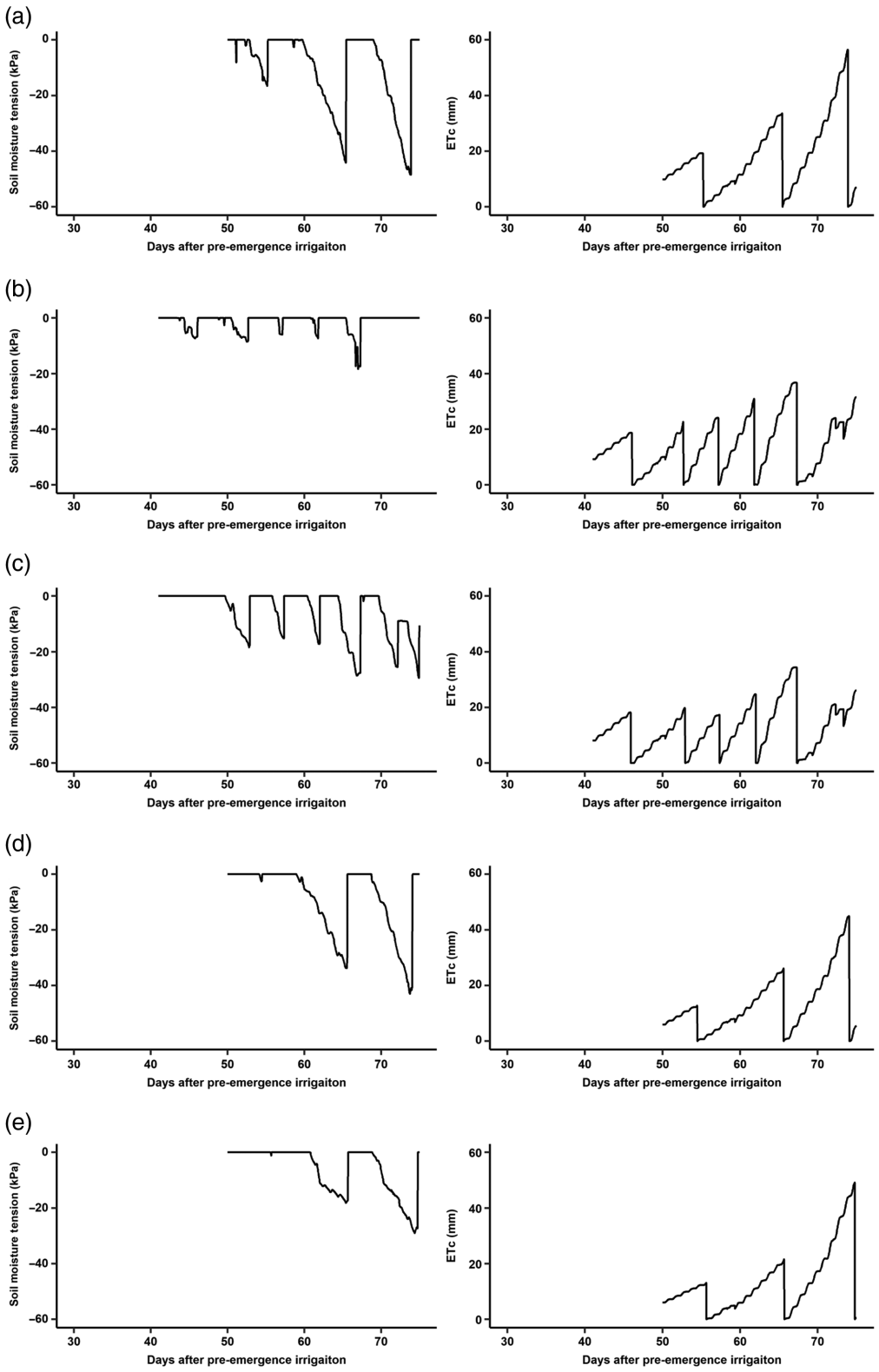

Fig. 4 Left: SMT (kPa) and right: ETc with rainfall subtracted (mm), in relation to number of days since pre-emergent irrigation with letters (a)–(e) used to distinguish individual replicate data from year 2. Note: IoT loggers to monitor SMT were not installed until establishment; hence data in the establishment phase is not presented.

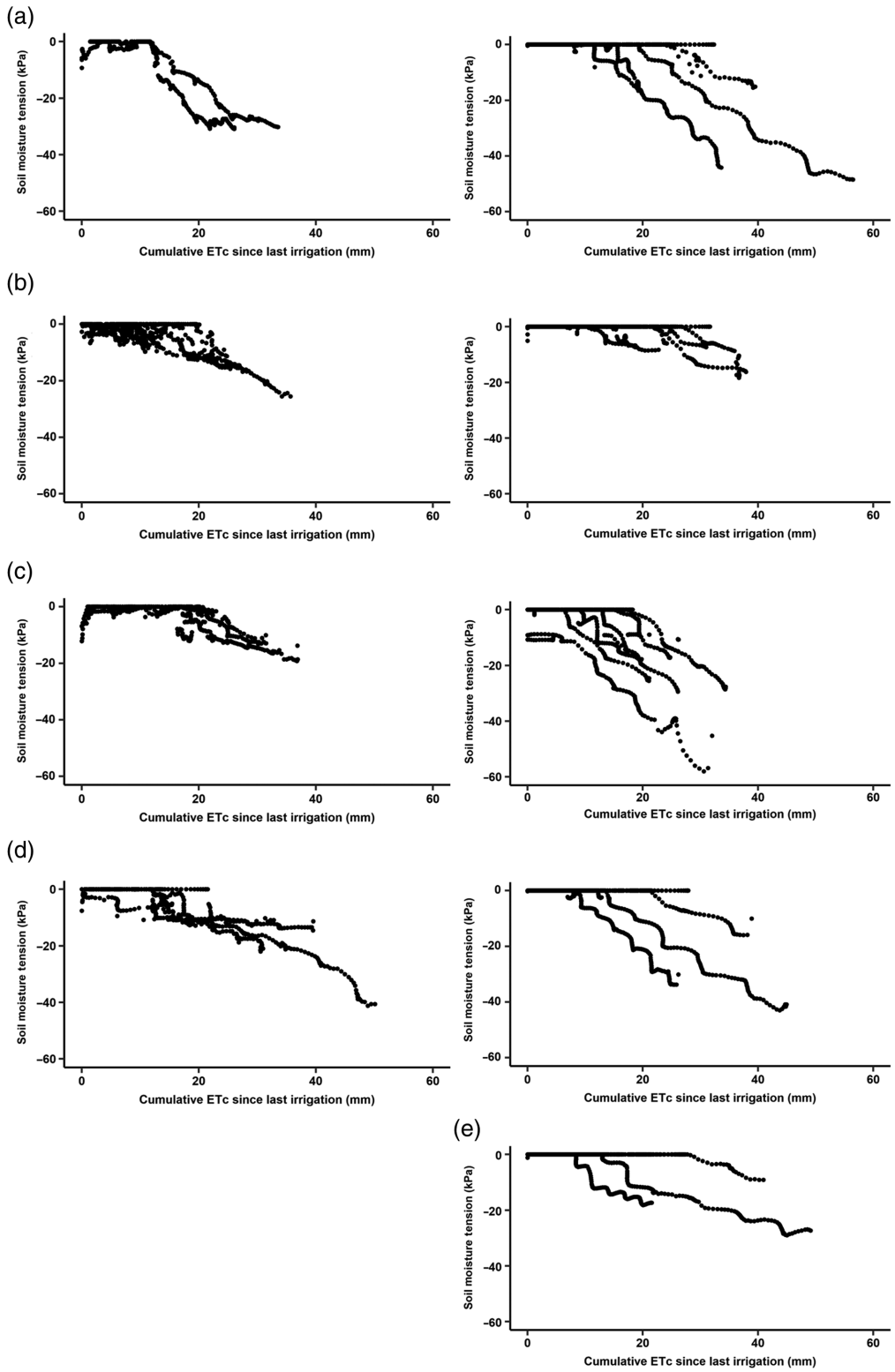

Fig. 5 (a)–(e) Relationship between SMT (kPa) and cumulative ETc with rainfall subtracted (mm) since last irrigation for each replicate. Data from year 1 is presented on the left, and year 2 is on the right.

soil evaporation is highest in wet soils and decreases with declining moisture availability.[43] The gradient of the linear relationship (m) between SMT and cumulative ETc of −1.0 implies that, for every mm increase in ETc beyond c, SMT declined 1.0 kPa. However, to build a predictive model, determination of the cumulative ETc when m can be applied (point c) is required.

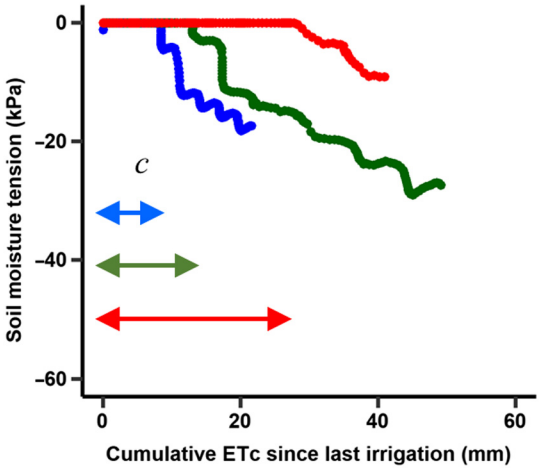

Fig. 6 Example of the relationship between SMT and cumulative ETc (mm) since last irrigation with different colors used to show how the point of inflection (c) increases throughout the season. (blue = 55, green = 65, and red = 84 days after pre-emergent irrigation).

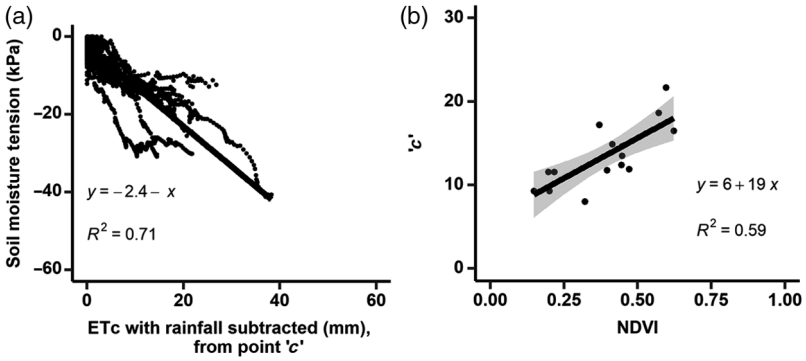

Fig. 7 a) Translated graph of SMT (kPa) and ETc with rainfall subtracted (mm) from point c (kPa < −1). Each line represents a deficit period that has been translated c units horizontally with data from all replicates included from year 1. (b) "c" versus NDVI in year 1, demonstrating the relationship between canopy cover and the cumulative ETc at which soil moisture begins to decline.

Due to increasing canopy cover slowing the rate of soil evaporation and increasing the time taken for soil to transition from saturated to non-saturated (when soil evaporation is the major influence of soil water decline),[32,43] NDVI was used as a proxy measure to account for the change in canopy cover experienced throughout the season. As hypothesized, c was found to be correlated to NDVI values [$R^2 = 0.59$, Fig. 7(b)].

Using the relationship between ETc and SMT [m, Fig. 7(a)], and the point at which SMT declines [c, Fig. 7(b)], a model to predict SMT was obtained by adding the point of inflection to the product of m and cumulative ETc since last irrigation (with rainfall subtracted) according to the following equation:

$$\text{Soil moisture tension (kPa)} = m \times \text{ETc (mm)} + c, \text{ if SMT} > 0, = 0, \tag{5}$$

where m is a constant (determined in this soil type under mild to moderate soil moisture deficit during the post-establishment to PI period to equal −1.0) and c represents the period after irrigation at which soil moisture begins to decline according to the equation

$$c = 19 \times \text{NDVI} + 6. \tag{6}$$

3.3 Assessment of Model to Predict Soil Moisture Tension

To assess the robustness of the model across seasons, remote sensed ETc and NDVI data collected from individual replicates in year 2 was used to predict SMT according to Eq. (5) and

compared with the measured values presented in Fig. 4. The accuracy of the predicted SMT for the five individual replicates and all data combined is provided in Fig. 8.

The model developed from data collected in year 1 to predict SMT of five replicates in year 2 achieved an R^2 ranging from 0.40 to 0.88 with the combined data achieving 0.70 [Fig. 8(f)]. Of greater importance is the RMSE, which ranged from ±3.5 to ±7.0 kPa in the individual replicates with the combined RMSE ±5.8 kPa (Table 1). The reduced accuracy of the model in replicate *C* is potentially due to soil and therefore crop variability within the area immediately surrounding the SMT sensor. In this area only, a water reservoir previously existed prior to recent filling with coarser textured soil. The model can be seen to underestimate the extent of soil moisture deficit, with the increased frequency of soil moisture deficit events likely a result of the lower water holding capacity in this particular area. This highlights the limitation of the model to be used in other soil types. Although the area was not ideal for SMT sensor placement, this location was selected as the same IoT logger was used to monitor water progress down the replicate during an irrigation event and was required in this location to ensure full irrigation of the replicate while minimizing excessive run-off. This highlights the limitation of point-based sensing as it may not have adequately represented the 900 m^2 area in which the spectral indices were calculated.

The combined RMSE of ±5.8 kPa is considered sufficient for scheduling irrigation in a commercial environment. However, it must be highlighted that after an irrigation event, SMT

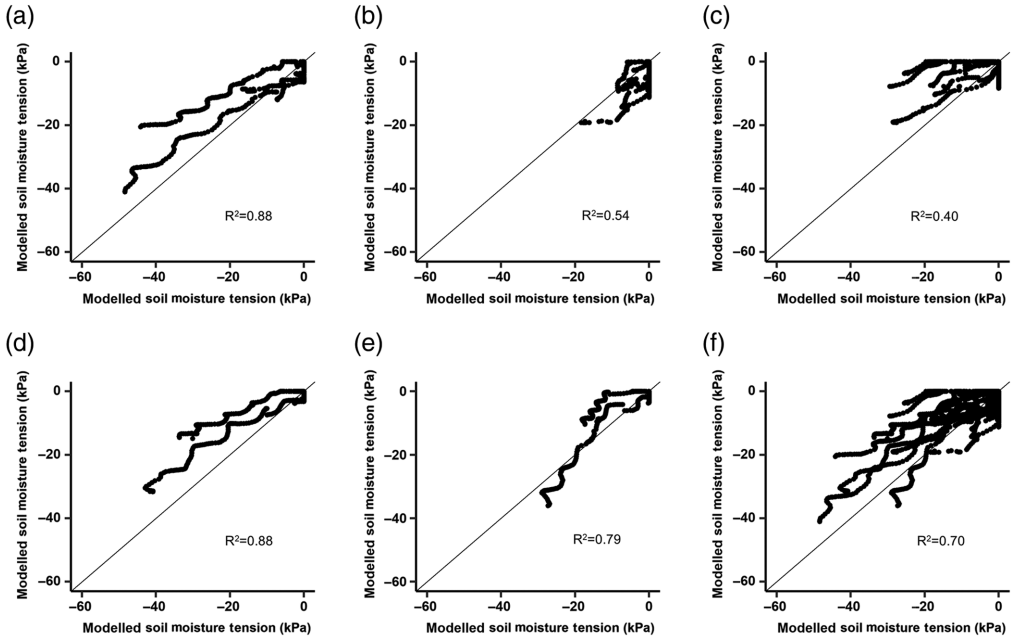

Fig. 8 Actual versus predicted SMT in year 2 of five individual replicates (a)–(e) and all data combined from the five replicates presented in panel (f) with a 1:1 line included for perspective. The model was developed from data collected in year 1.

Table 1 Individual replicate (A–E) and all data combined (F) R^2 and RMSE values 0 to −10 kPa, < − 10 kPa and overall, for forecast SMT in year 2 using the model built from year 1 data.

		A	B	C	D	E	Combined
R^2		0.88	0.54	0.40	0.88	0.79	0.70
RMSE	>−10 kPa	2.4	3.5	3.1	2.3	1.6	2.8
	<−10 kPa	11.2	4.8	12.2	11.9	6.9	10.7
	Overall	6.7	3.5	7.0	6.9	4.1	5.8

returned to 0 kPa and remained at or close to that value for some time. Therefore, many measured data points were 0 kPa (58%), with 76% of data points occurring under saturated conditions (0 to −10 kPa). Accuracy beyond −10 kPa is of greater importance for irrigators as this is when irrigation decisions are required. RMSE calculated separately for 0 to −10 kPa and beyond −10 kPa is provided in Table 1. From 0 to −10 kPa, the RMSE was ±2.8 kPa and ±10.7 kPa for SMT beyond −10 kPa when all replicate data were combined.

3.4 Evaluation and Limitations of the Model

The model is shown in Fig. 8 to under-estimate SMT in year 2, indicating that the rate of soil moisture decline in year 2 was greater than in year 1. A comparison between year 1 and year 2 on the rate of soil moisture decline in relation to ETc is shown in Fig. 9, where the gradient, m, in year 1 was −1, but in year 2 it was found to be −1.4. For every mm increase in ETc beyond c, SMT declined 1.4 kPa in year 2, as opposed to 1.0 kPa in year 1.

The different rate of SMT decline is likely a result of the residual stubble from the winter cereal grown prior to rice in year 1 acting as a mulching layer to slow the exchange of water between the soil and atmosphere by buffering the soil surface temperature, reducing the heat flux, and therefore reducing soil evaporation losses in year 1.[32] Rice stubble was burned prior to seeding in year 2, a practice known to increase soil evaporation.[44] This highlights the impact of management practices on soil moisture and therefore a limitation of the model for widespread adoption.

Furthermore, decreasing the frequency of irrigation (extending the SMT beyond the −40 kPa reported here) would likely further increase the rate of decline in SMT compared with ETc due to increased resistance of moisture movement associated with declining soil water.[32,43] However, increasing soil moisture deficit beyond the values analyzed in the current study was found to have adverse yield implications and is not recommended in a temperate Australian environment, as reported in Ref. 25. Nevertheless, the model proved to estimate SMT within an overall RMSE of ±5.8 kPa and is considered appropriate to schedule irrigation in this environment. Short term (7-day) ET_0 forecasts are considered reasonably accurate in the region, providing opportunity for future research to incorporate forecast ET_0 into the model to predict SMT multiple days in advance. This would enable forward scheduling of irrigation, which is required when irrigation water is not available on demand and water ordering requires a lead time. Such forecasting has been demonstrated for use in cotton production by Refs. 36 and 45 and offers potential to be incorporated into an automated irrigation system for water saving rice production. Although generally not an issue in semi-arid regions, cloud cover may limit the accuracy of predictions, with increased frequency of imagery preferable. This may be possible with the incorporation of other satellite-based sensing alternatives; however, the fusion

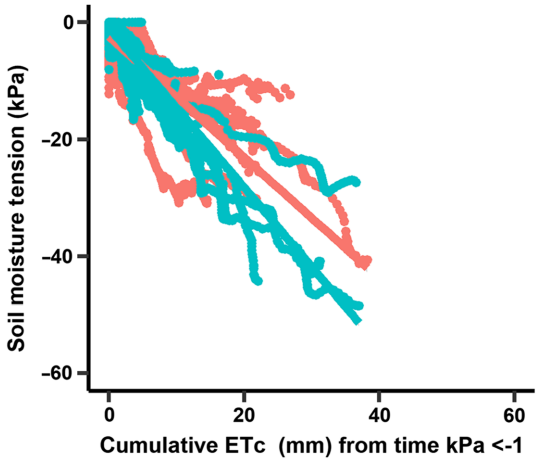

Fig. 9 Translated graph of SMT (kPa) and ETc with rainfall subtracted (mm) from the time kPa < −1. Each line represents a deficit period that has been translated c units horizontally with data from all replicates included from year 1 in red and year 2 in blue.

of spectral indices may be required to ensure that properly calibrated NDVI values can be achieved.

4 Conclusion

This manuscript presents the relationship between SMT and cumulative crop evapotranspiration (with rainfall subtracted) as calculated using remote sensed satellite data for non-ponded aerobic rice grown in heavy clay soil in temperate Australia. Using remote sensed data collected from a commercial rice field, a model was developed to predict SMT of an independent dataset with an RMSE of ± 5.8 kPa. This offers the potential for irrigators to schedule irrigation using open access, free data, without the need for costly in-field sensors. Further benefit to rice farmers may be gained from future research to incorporate short-term forecast crop evapotranspiration and therefore SMT, providing irrigators more time to plan irrigation activities.

Code, Data, and Materials Availability

The data presented in this study are available on request from the corresponding author.

Acknowledgments

This project received funding from the Australian government's Future Drought Fund. The authors acknowledge Darrell Fiddler and DeBortoli Wines for providing the trial site and for their assistance throughout the study. The authors declare no conflicts of interest.

References

1. B. A. M. Bouman and T. P. Tuong, "Field water management to save water and increase its productivity in irrigated lowland rice," *Agric. Water Manage.* **49**, 11–30 (2001).
2. G. Carracelas et al., "Irrigation management strategies to increase water productivity in *Oryza sativa* (rice) in Uruguay," *Agric. Water Manage.* **222**, 161–172 (2019).
3. D. R. Carrijo et al., "Impacts of variable soil drying in alternate wetting and drying rice systems on yields, grain arsenic concentration and soil moisture dynamics," *Field Crop. Res.* **222**, 101–110 (2018).
4. J. L. Chlapecka et al., "Scheduling rice irrigation using soil moisture thresholds for furrow irrigation and intermittent flooding," *Agron. J.* **113**, 1258–1270 (2021).
5. S. K. De Datta, W. P. Abilay, and G. N. Kalwar, "Water stress effects in flooded tropical rice," in *Water Management in Philippine Irrigation Systems: Research and Operations*, pp. 19–36, IRRI, Los Banos, Philippines (1973).
6. B. Dunn and D. Gaydon, "Rice growth, yield and water productivity responses to irrigation scheduling prior to the delayed application of continuous flooding in South-East Australia," *Agric. Water Manage.* **98**(12), 1799–1807 (2011).
7. A. Froes et al., "Aerobic rice system improves water productivity, nitrogen recovery and crop performance in Brazilian weathered lowland soil," *Field Crop. Res.* **218**, 59–68 (2018).
8. S. Hatta, "Water consumption in paddy field and water saving rice culture in the tropical zone," *Jpn. J. Trop. Agric.* **11**(3), 106–112 (1967).
9. Y. Kato, M. Okami, and K. Katsura, "Yield potential and water use efficiency of aerobic rice (*Oryza sativa* L.) in Japan," *Field Crop. Res.* **113**(3), 328–334 (2009).
10. Sudhir-Yadav et al., "Effect of water management on dry seeded and puddled transplanted rice. Part 1: crop performance," *Field Crop. Res.* **120**(1), 112–122 (2011).
11. D. F. Tabbal, R. M. Lampayan, and S. I. Bhuiyan, "Water-efficient irrigation technique for rice," in *Soil and Water Engineering for Paddy Field Management*, AIT, Bangkok, Thailand, pp. 146–159 (1993).
12. Y. Xiaoguang et al., "Performance of temperate aerobic rice under different water regimes in North China," *Agric. Water Manage.* **74**, 107–122 (2005).
13. T. K. Adhya et al., "Wetting and drying: reducing greenhouse gas emissions and saving water from rice production," World Resour. Inst. 1–28 (2014).
14. B. A. M. Bouman et al., "Rice and water," *Adv. Agron.* **92**, 187–237 (2007).
15. G. LaHue et al., "Alternate wetting and drying in high yielding direct-seeded rice systems accomplishes multiple environmental and agronomic objectives," *Agric. Ecosyst. Environ.* **229**, 30–39 (2016).
16. B. A. Linquist et al., "Reducing greenhouse gas emissions, water use, and grain arsenic levels in rice systems," *Glob. Chang. Biol.* **21**(1), 407–417 (2015).
17. L. C. Guerra et al., "Producing more rice with less water from irrigated systems," Int. Water Manage. Inst. SWIM Paper, 1–33 (1998).

18. R. M. Lampayan et al., "Field crops research adoption and economics of alternate wetting and drying water management for irrigated lowland rice," *Field Crop. Res.* **170**, 95–108 (2015).
19. B. A. M. Bouman, R. M. Lampayan, and T. P. Tuong, *Water Management in Irrigated Rice: Coping with Water Scarcity*, International Rice Research Institute, Los Baños, Philippines (2007).
20. S. S. Kukal, G. S. Hira, and A. S. Sidhu, "Soil matric potential-based irrigation scheduling to rice (*Oryza Sativa*)," *Irrig. Sci.* **23**(4), 153–159 (2005).
21. H. Zhang et al., "An alternate wetting and moderate soil drying regime improves root and shoot growth in rice," *Crop Sci. Soc. Am.* **49**, 2246–2260 (2009).
22. K. Djaman et al., "Effects of alternate wetting and drying irrigation regime and nitrogen fertilizer on yield and nitrogen use efficiency of irrigated rice in the Sahel," *Water* **10**(6), 711 (2018).
23. T. P. Tuong, B. A. M. Bouman, and M. Mortimer, "More rice, less water—integrated approaches for increasing water productivity in irrigated rice-based systems in Asia," *Plant Prod. Sci.* **8**(3), 231–241 (2005).
24. S. Fukai and L. J. Wade, "Rice," in *Crop Physiology: Case Histories for Major Crops*, V. Sadras and D. Calderini, Eds., pp. 44–97, Elsevier Inc. (2021).
25. M. Champness, C. Ballester, and J. Hornbuckle, "Effect of soil moisture deficit on aerobic rice in temperate Australia," *Agronomy* **13**(168), 18 (2023).
26. S. K. Chaudhary and P. K. Srivastava, *Future Challenges in Agricultural Water Management*, Elsevier Inc. (2021).
27. H. G. Jones, "Monitoring plant and soil water status: established and novel methods revisited and their relevance to studies of drought tolerance," *J. Exp. Bot.* **58**(2), 119–130 (2007).
28. S. Irmak et al., *Principles and Operational Characteristics of Watermark Granular Matrix Sensor to Measure Soil Water Status and Its Practical Applications for Irrigation Management in Various Soil Textures*, Vol. 783, Lincoln (2016).
29. "Soil moisture contents," in *Advanced Remote Sensing*, S. Liang and J. Wang, Eds., pp. 685–711, Academic Press (2020).
30. J. Hornbuckle et al., "IrriSAT technical reference," https://irrisat-cloud.appspot.com/doc/IrriSAT_Technical_Reference.pdf (accessed 12 December 2022).
31. R. Allen et al., "EEFlux: a landsat-based evapotranspiration mapping tool on the Google Earth Engine," in *ASABE Irrig. Symp.*, ASABE, Long Beach, CA, USA, Vol. 701P0415 (2015).
32. R. Allen et al., "Crop evapotranspiration-guidelines for computing crop water requirements," FAO Irrigation and Drainage Paper 56, Vol. 56, FAO – Food and Agriculture Organization of the United Nations, Rome (1998).
33. T. J. Trout and L. F. Johnson, "Estimating crop water use from remotely sensed NDVI, crop models, and reference ET," in *USCID Fourth Int. Conf. Irrig. and Drain.*, Sacramento, California, pp. 275–285 (2007).
34. J. Bellvert et al., "Monitoring crop evapotranspiration and crop coefficients over an almond and pistachio orchard throughout remote sensing," *Remote Sens.* **10**(12), 2001 (2018).
35. M. Odi-Lara et al., "Estimating evapotranspiration of an apple orchard using a remote sensing-based soil water balance," *Remote Sens.* **8**(3), 253 (2016).
36. R. Filev Maia, C. Ballester Lurbe, and J. Hornbuckle, "Machine learning approach to estimate soil matric potential in the plant root zone based on remote sensing data," *Front. Plant Sci.* **13**, 1–16 (2022).
37. J. Hornbuckle and E. Christen, "Physical properties of soils in the murrumbidgee and coleambally irrigation areas," CSIRO L. Water Tech. Rep. 17, 175 (1999).
38. E. Humphreys et al., "Integration of approaches to increasing water use efficiency in rice-based systems in Southeast Australia," *Field Crop. Res.* **97**, 19–33 (2006).
39. J. Brinkhoff, J. Hornbuckle, and T. Dowling, "Multisensor capacitance probes for simultaneously monitoring rice field soil-water- crop-ambient conditions," *Sensors* **18**(1), 1–14 (2017).
40. Technical Committee on Standardization of Reference Evapotranspiration, *The ASCE Standardized Reference Evapotranspiration Equation*, R. Allen et al., Eds., ASCE (2005).
41. W. Rouse et al., "Monitoring vegetation systems in the great plains with ERTS," in *Third Earth Resour. Technol. Satellite-1 Symp. – Vol. I: Tech. Present.*, S. Freden, E. Mercanti, and M. Becker, Eds., NASA, Goddard Space Flight Center, Washington, DC, pp. 309–317 (1974).
42. P. K. Thapliyal et al., "Improvement in the retrieval of humidity profiles using hybrid regression technique from infrared sounder data: a simulation study," *Meteorol. Appl.* **21**(2), 301–308 (2014).
43. W. A. Jury and R. Horton, *Soil Physics*, 6th ed., John Wiley & Sons, Inc., New York (2004).
44. H. S. Sidhu et al., "The happy seeder enables direct drilling of wheat into rice stubble," *Aust. J. Exp. Agric.* **47**(7), 844–854 (2007).
45. J. Brinkhoff, J. Hornbuckle, and C. Ballester Lurbe, "Soil moisture forecasting for irrigation recommendation," *IFAC-PapersOnLine* **52**(30), 385–390 (2019).

Matthew Champness is has submitted his PhD at Deakin University. He received his BS degree (Hons I) in agricultural science from Charles Sturt University. His current research interests include water saving irrigation and methane mitigation from rice paddy to improve water productivity and sustainability of agricultural practices. He has a keen interest in improving farmer livelihoods through enhanced agricultural practices.

Biographies of the other authors are not available.